# CHAPTER III

## X-RAY STUDIES ON THE SMECTIC A PHASE EXHIBITED BY SEVERAL STRUCTURALLY RELATED COMPOUNDS

### 3.1 Introduction

The smectic A phase is characterized by a layered arrangement of rod like molecules, the long axis of the molecules being on the average normal to the smectic planes, though there is a random distribution of molecular centres within each layer. Xray diffraction pattern of a polydomain smectic A sample has a large angle diffuse ring which corresponds to the mean intermolecular distance normal to the director and is indicative of liquid like arrangement within the layers. In addition, there is a sharply defined low angle ring which corresponds to the periodicity along the layer normal (layer thickness or layer spacing). These aspects concerning Xray diffraction pattern have already been discussed in detail in chapter I.

Intuitively, one expects the layer spacing in the smectic A phase to be approximately equal to the molecular length. This seems to be true in the case

of compounds consisting of weakly polar molecules.[1] However, the layer spacing is found to be much larger than the molecular length in compounds whose molecules have a strongly polar terminal group.[1] This structure arises from the antiparallel correlations between neighbouring molecules brought about by the strong dipole moments.[2]

A typical mesogenic molecule has a rigid central core which is often aromatic with flexible alkyl chains at one or both the ends. Generally speaking, the lower homologues show only the nematic phase. The smectic phase is exhibited by homologues with relatively longer chain lengths, the number of carbon atoms (n) in the chains being usually seven or higher. As n increases, the nematic range is decreased, and beyond a certain chain length, the nematic phase disappears and transition takes place directly from the smectic to the isotropic phase. As we noted in chapter I, these observations have been accounted for on the basis of the fact that the strongest part of the intermolecular attractions occurs between aromatic cores of the molecules. Obviously for molecules with long aliphatic end chains, the interactions between aromatic cores leads to the formation of a layered organization of the molecules, characteristic of smectic phases.

McMillan[3] proposed a molecular theory of the A phase which is an extension of the Maier-Saupe's theory of nematics,[4] taking into account the density wave along the director.

Longitudinal components of strong permanent dipolar groups of mesogenic molecules are now known to make an important contribution to the stability of the N and A phases.[5] Xray and neutron diffraction studies[1,6,7] on cyanobiphenyls showed that the layer spacing is $\simeq 1.4$ molecular length. A bilayer structure, as indicated in fig.1.7 (chapter I), was proposed to account for these observations.[1] As a result of the attractive interactions between the neighbouring molecules, aromatic cores overlap in the middle of the layers and the alkyl chains extend outward. This arrangement of the molecules is called bilayer, or more appropriately, partial bilayer structure (fig.1.7). The structure of the (partial) bilayer gives an extra degree of freedom to such systems and leads to several interesting phenomena like reentrance[8-10] and smectic A polymorphism.[5]

The structure of the bilayer depends on the chemical structure of the aromatic core. It is found

to depend on the mutual disposition of all the dipolar groups that the cores may possess. As was discussed by the Bordeaux group, if the dipole moments of the linkage groups in the aromatic core oppose that of the terminal group, the compounds exhibit large bilayer spacings. For instance, DB5, 4-n-pentyl phenyl-4'-(4"-cyanobenzoyloxy)benzoate, has a layer spacing in the smectic A phase $\simeq 2l$, $l$ being the molecular length.[11] On the other hand, if the dipole moments of the bridging groups in the aromatic core are aligned in the direction of the dipole moment of the terminal polar group, the compounds have a bilayer spacing $\simeq 1.4\,l$ in the $A$ phase which is designated as $A_d$ phase according to the nomenclature introduced by Levelut et al.[12] Some compounds having the $A_d$ phase also exhibit reentrant phases. The 11$^{th}$ and 12$^{th}$ members of the series 4-cyanophenyl-3'-methyl-4'-(4"-n-alkylbenzoyloxy)benzoates (nCPMB) synthesized in our laboratory some years ago were amongst the first compounds which exhibited the reentrant nematic phase at atmospheric pressure.[9] These compounds have two ester linkage groups with their dipoles oriented parallel to the end cyano dipoles, and further, have a lateral methyl group (fig. 3.1).

In order to study the effect of reversing the ester dipoles in relation to that of the cyano end group of the above compounds, 4-n-alkyl phenyl-3'-methyl-4'-(4"-n-cyanobenzoyloxy)benzoates (nP*MCBB), their nitro analogues, and other structurally related compounds were synthesized in our laboratory. In this chapter, we present the thermal evolution of layer spacings in the A phase of these compounds. Indeed because of the bulky lateral substituents (methyl or methoxy) the intermolecular interactions are weakened compared to compounds without such lateral substituents. As we shall find in this and the next chapters, the lateral substitution results in some new features in the temperature variations of the physical properties of these compounds.

## 3.2 Experimental

### (i) Materials

All the compounds were synthesized in our chemistry laboratory.[13,14] The transition temperatures were determined by using a Mettler hot stage (Model FP52) in conjunction with a polarizing microscope, as well as a differential scanning calorimeter (Perkin Elmer DSC-2). The heats of transitionswere determined from the DSC

traces. The transition temperatures and heats of transitions are listed in table 3.1. The structural formulae and acronyms of the compounds are shown in fig. 3.1.

(ii) Sample Holder and Heater

The sample holder and the heater used to maintain the temperature of the sample at any desired value are shown in fig. 3.2.

heater (fig. 3.2b) consisted of a circular copper rod having a rectangular slot along its length. The central portion of the rod was machined to have a rectangular cross section so as to facilitate mounting between the pole pieces of a permanent magnet. Nichrome wire was wound on the bottom and top circular parts of rod on a mica sheet used as insulator. A tapered ($O_1$) was drilled at the centre of the heater, and perpendicular to its long dimension for the Xrays to pass through. The tapered hole had a small diameter of 0.6 mm to collimate the Xray beam at the entrance side. The conical angle of the exit aperture was about $45^{o}$, which was more than adequate for the Xray diffraction studies of our compounds.

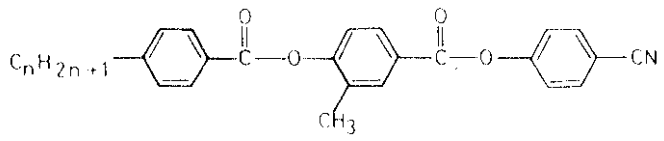

4 - cyanophenyl – 3′ – methyl – 4′-(4″–n – alkyl benzoyloxy) benzoates

(nCPMBB)

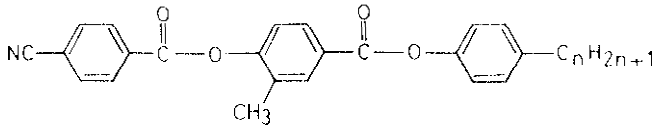

4 -n – alkylphenyl - 3′ - methyl –4′– (4″–cyanobenzoyloxy) benzoates

(nPMCBB)

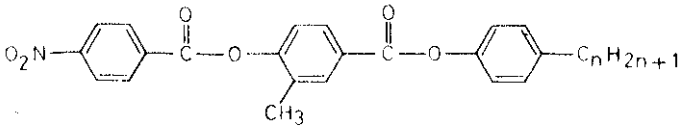

4 – n – alkylphenyl – 3′– methyl –4′–(4″–nitrobenzoyloxy) benzoates

(nPMNBB)

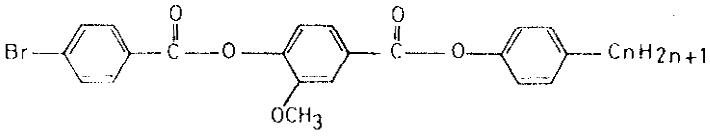

4 - n - alkylphenyl - 3′ - methoxy - 4′ - (4″ - bromobenzoyloxy) benzoates

(nPMeOBrBB)

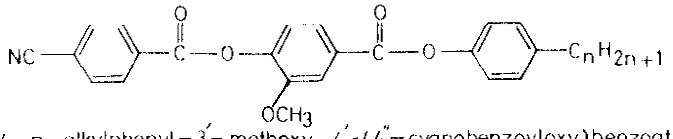

4 – n alkylphenyl – 3′– methoxy 4′-(4″–cyanobenzoyloxy)benzoates

(nPMeoCBB)

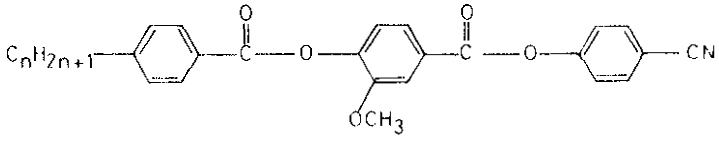

4 - cyanophenyl – 3′ - methoxy - 4′ - (4″ - n - alkyl benzoyloxy ) benzoates

(nCPMeOBB)

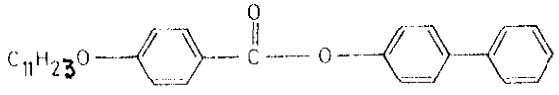

4 - biphenylyl - 4″ - n - undecyloxy benzoate

(BO11)

**FIG.3.1: Structural formulae and acronyms of various compounds used in our investigations**

The sample holder (fig. 3.2a) consisted of a long rectangular copper strip ('lip') which fitted exactly into the rectangular slot of the heater. This enabled us to place the sample holder in the same position every time the sample was mounted. Consequently the sample to film distance remained constant in a given series of experiments. The lip had a hole ($O_2$) of 0.6 mm diameter along the wider side and at an appropriate height. Through this hole a Lindemann capillary tube containing the sample could be inserted. The lip also had a tapered hole ($O_3$) at right angles to the hole for the capillary, the former matching with the hole ($O_1$) on the outer jacket of the heater. This was used for the passage of Xrays through the sample. 6 μm thick mylar sheets were pasted on both sides of the tapered hole ($O_1$) on the outer heater to prevent air currents and thereby avoiding temperature fluctuations of the sample.

The heater was kept between the pole pieces of a permanent magnet (NS) of strength 4 KGauss such that the sample position was at the centre of the pole pieces and the field was normal to the incident Xray beam. The heater and the magnet assembly were mounted on a stand of adjustable height.

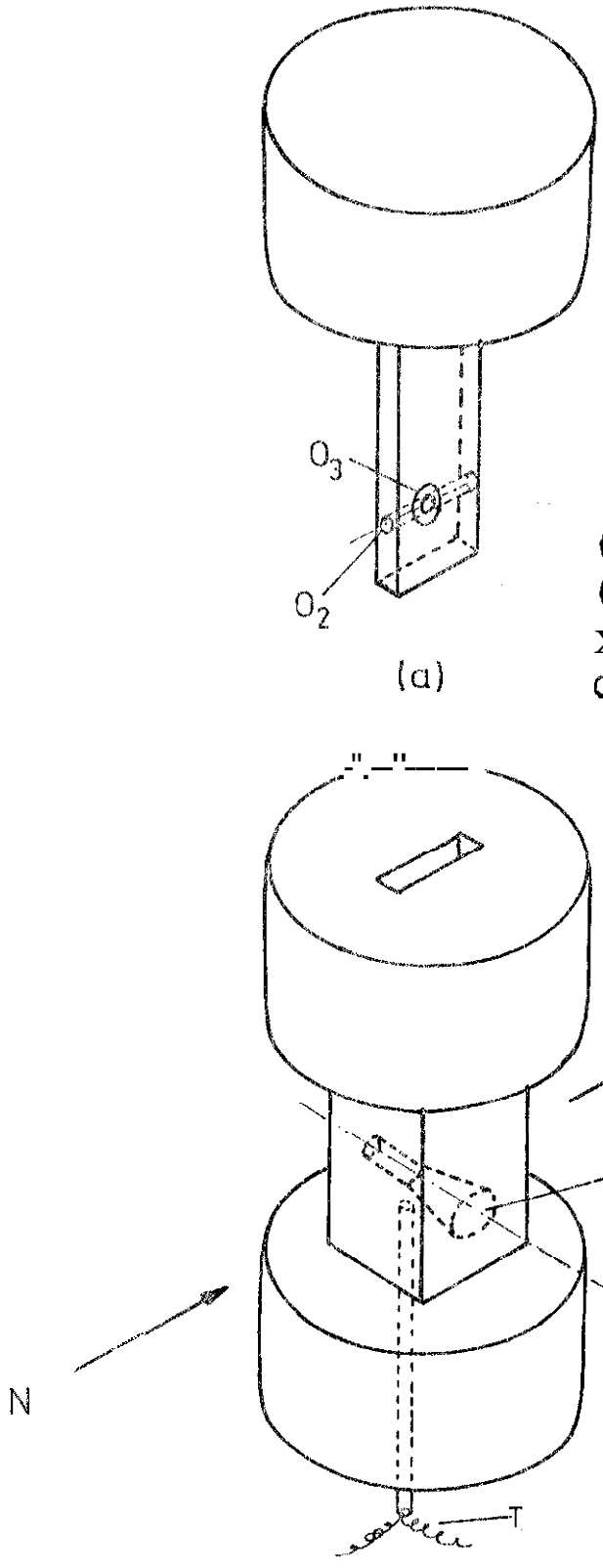


FIG.3.2

(a) Sample holder, and
(b) Beater used for Xray studies.

$O_1$ - tapered hole for the passage of Frays.

$O_2$ - hole for the inaertion of the capillary tribe.

$O_3$ - hole for the passage of Xrays.

T - thermocouple

NS - Direction of the magnetic field

The temperature of the sample could be adjusted to any desired value by varying the current through the heater using a highly stabilized power supply (Digireg 233).

(iii) Temperature measurement

A copper-constantan thermocouple (T) was inserted into the heater from the bottom such that the junction was as close as possible to the sample. The thermo e.m.f. was measured with a $4\frac{1}{2}$ digit panel meter (Yamuna 1008A). The thermocouple was calibrated by taking standard samples in the Lindemann capillary tubes and observing their transitions visually. Temperature of the sample could be measured and maintained to an accuracy of $\pm 0.25^{\circ}C$ over long periods of time.

(iv) Xray Studies

After filling the Lindemann capillary tube with the sample, the ends of the tubes were sealed. The tube was mounted in the sample holder in a position perpendicular to the incident Xray beam. The sample was irradiated with monochromatic $CuK_{\alpha}$ radiation coming from W1730 Phillips Xray Generator and a bent quartz crystal monochromator (Carl-Zeiss Jena). The sample

was heated to the nematic phase and slowly cooled in the presence of a magnetic field of strength 4 KGauss to get aligned samples in the smectic A phase. The diffracted Xray beam was collected on a flat film kept at a distance of approximately 30 cm from the sample. The exposure time varied from 10 min. to one hour depending on the sample under investigation. After the completion of the experiment, transition temperature of the sample was remeasured and found to be unaltered within the limits of experimental error indicating that the sample did not deteriorate during the exposure time.

The sample to film distance was standardized by using the (100) reflection of p-decanoic acid, the d value of this reflection being taken to be 23.1 Å.[15] The distance between the diffraction spots on the film was measured using an accurate comparator (Adam-Hilger Ltd.). The accuracy of layer spacing measurement was generally ±0.1 Å.

## 3.3 Results and Discussion

### (1) Thermodynamic Properties

The structural formulae and acronyms of the compounds of interest are shown in fig.3.1. The molecules

of nCPMBB have two ester groups whose dipole moments are parallel to that of the end cyano group. The 11$^{th}$ and 12$^{th}$ members of this series exhibit smectic A and reentrant nematic phases.[9] nPMCBB compounds are obtained by interchanging the two end groups of nCPMBB so that the longitudinal components of the two ester groups are now antiparallel with the terminal cyano group. It is interesting to note that the molecular cores of the resulting nPMCBB compounds are very similar to that of DB5 compound whose homologues have been extensively studied by the Bordeaux group[11,16] except that a lateral methyl substituent is now attached to the core. We have also studied several structurally related compounds (fig.3.1) and present a detailed comparative study of them. We have studied only a few higher homologues in each series, since our main interest was to investigate the A phase.

From table 3.1, we see that (a) nPMCBB compounds melt at much lower temperatures than the corresponding nCPMBB compounds; (b) an enantiotropic A phase appears at the ninth member of nPMCBB while 11 CPMBB is the lowest homologue which exhibits the A phase; (c) both AN (smectic A-nematic) and NI (nematic-isotropic)

transition temperatures of 12 PMCBB are higher than the corresponding temperatures of 12 CPMBB; (d) while nCPMBB with n = 11 and 12 exhibit a reentrant nematic phase, there is no such reentrant phase in the case of nPMCBB; (e) the DSC run of 10 PMCBB shows a slope change at 124.5°C indicating a phase transition at that temperature. However, interestingly under a polarizing microscope, the same A phase texture is found both above and below 124.5°C.

Comparing the transition temperatures of nPMMBB with those of nPMCBB, the former have higher melting points but lower A-N and N-I transition points. Replacement of the lateral methyl substituent of nPMCBB and nCPMBB by the bulkier methoxy group results in higher melting points of nPMeOCBB and nCPMeOBB, but considerably lower A-N and N-I transition points. The latter results can be attributed to the weakening of the intermolecular interactions resulting from the bulkier side group of nPMeOCBB and nCPMeOBB molecules. Unlike in the nCPMBB series, none of the nCPMeOBB compounds show reentrant phases. Comparing nPMeOCBB and nPMeOBrBB, we see that the latter compounds have slightly lower melting points and show monotropic liquid crystalline phases.

## Table 3.1

Transition temperatures (in °C) and enthalpies of the compounds studied

| n | K | $N_R$ | A | N | I |
|---|---|---|---|---|---|
| | | nCPMBB[a] | | | |
| 11 | . 103 | (. 78.5) [0.0154] | . 127 [0.0147] | . 152.5 | . |
| 12 | . 102 | (. 59.8) [0.0464] | . 138.5 [0.0255] | . 148 | . |

| n | K | $A_2$ | $A_1$ | N | I |
|---|---|---|---|---|---|
| | | nPMCBB | | | |
| 9 | . 64.4 | | . 119.6 | . 175 | . |
| 10 | . 58 [14.1] | . 124.5 | . 139.5 [0.06] | . 169.5 [1.38] | . |
| 12 | . 67.5 [16.8] | . 77.1 | . 155.3 [0.42] | . 159.3 [1.48] | . |

| n | K | A | N | I |
|---|---|---|---|---|
| | | nPMNBB | | |
| 9 | . 75.9 [16.3] | (. 66.1) [0.019] | . 156.5 [1.11] | . |
| 10 | . 77.0 [21.6] | . 108.5 [0.062] | . 150.0 [1.13] | . |
| 12 | . 73.3 [20.0] | . 141.3 [0.165] | . 146.9 [1.28] | . |

Table 3.1 contd.

| n | K | A | N | I |
|---|---|---|---|---|
| | | nPMeOCBB | | |
| 10 | . 97.8 [33.7] | (. 94.4) | . 135.4 [1.56] | . |
| 11 | . 105 [35.1] | . 122 [0.035] | . 136 [1.8] | . |
| 12 | . 101.7 [28.8] | . 130.3 [0.21] | . 133.2 [1.7] | . |
| | | nOPMeOBB | | |
| 11 | . 121 [41.2] | . 130.1 [0.17] | . 133.3 [1.6] | . |
| 12 | . 122.8 [43.5] | . 131.7 | . 132.2 [3.13] | . |
| | | nPMeOBrBB | | |
| 11 | . 102.5 | (. 85.3) [0.26] | (. 95.6) [1.46] | . |
| 12 | . 93 [40.9] | (. 88.7) [0.29] | . 93.7 [1.43] | . |
| | | BO11[b] | | |
| | . 100.5 [53.2] | . 109.5 [1.4] | . 124.5 [0.9] | . |

The numbers in square brackets indicate enthalpies in kJ/mole. ( ) indicate monotropic transitions.

[a]Taken from ref. 9 [b]Taken from ref. 27.

(ii) Thermal evolution of layer spacings

The temperature variations of the layer spacings in 9PMCBB and 10 PMCBB are shown in figs.3.3 and 3.4 respectively. In both the cases, there is a large expansion of the layer as the temperature is decreased, the rate of expansion decreasing at lower temperatures. The molecular lengths of 9 PMCBB and 10 PMCBB calculated using Dreiding models are $\sim$31.8 and 33 Å respectively. Thus the measured layer spacing corresponds to 1.7$l$ and 1.6 $l$ close to $T_{AN}$ and increases to 1.86$l$ and 1.85$l$ ($l$ being the molecular length) at the lowest temperature before crystallization takes place in the 9$^{th}$ and 10$^{th}$ homologues respectively. More interestingly, a clear jump of $\sim$0.4 Å is observed in 10 PMCBB at $(T_{AN} - T) \simeq 15^{\circ}C$. The rate of increase in spacing slows down somewhat as the sample is cooled to this temperature, before the jump occurs (inset in fig. 3.4). The jump was confirmed by three independent trials. It corresponds to an A-A transition of the type found by the Bordeaux group in several cases.[16] The jump in the layer spacing is from $\sim$1.7$l$ to $\sim$1.72$l$. The lower temperature A phase gives rise to a relatively intense second order reflection, whose intensity increases with decrease of temperature. Positive prints of the

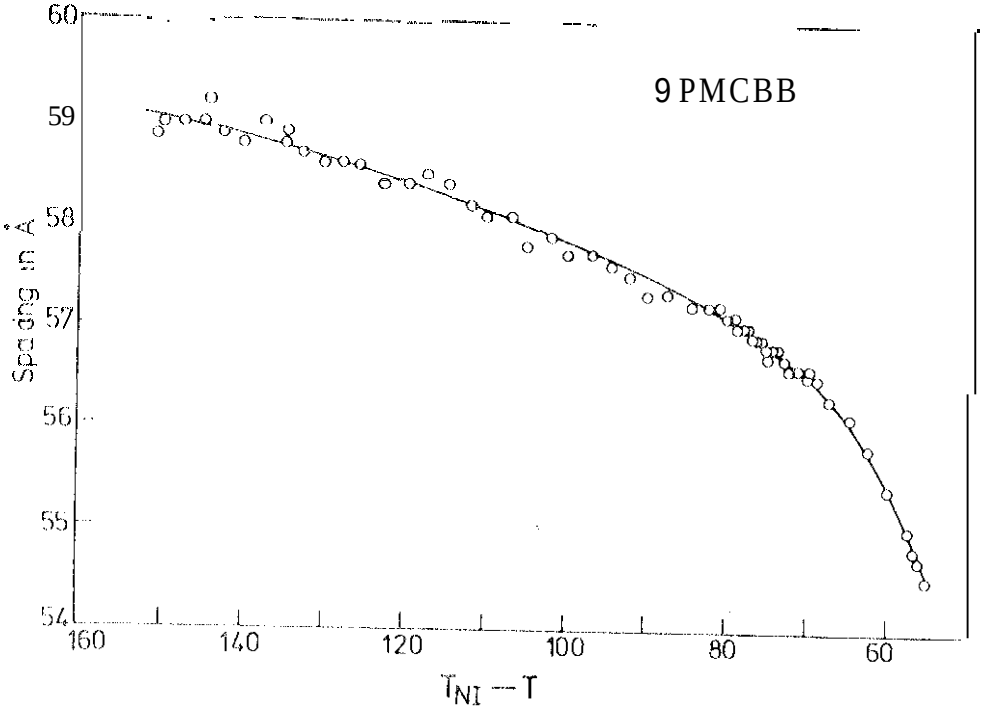


**FIGURE 3.3**

**Temperature variation of the Layer spacing of 9 PMCBB. ($T_{NI}$ - T) is the relative temperature, $T_{NI}$ being the nematic–isotropic transition temperature.**

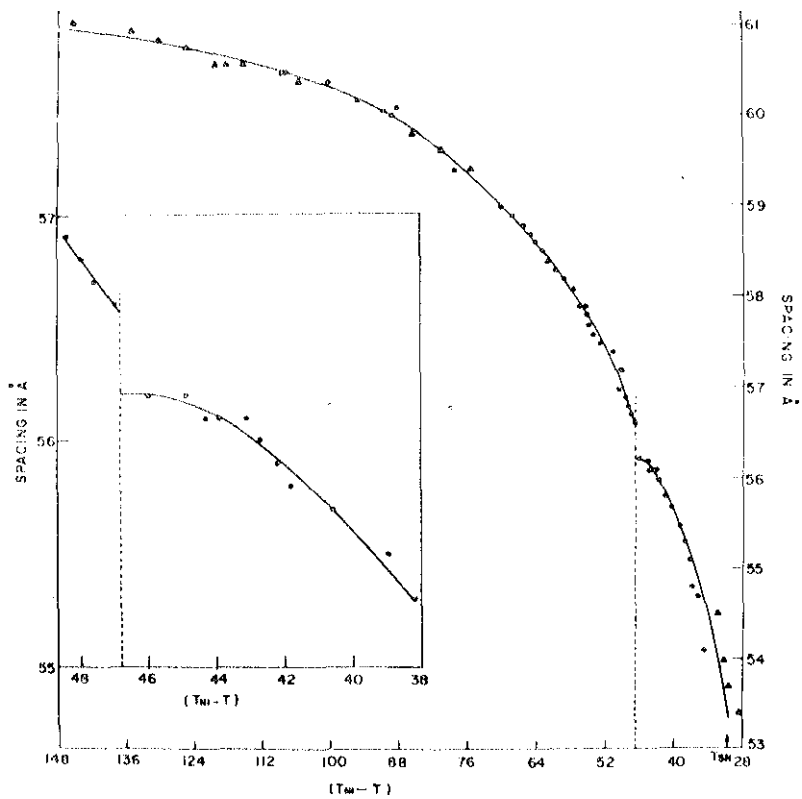


FIGURE 3.4

Temperature variation of the layer spacings of 10 PMCBB. ● and ▲ represent measurements accurate to ±0.1 Å and ±0.3 Å respectively. An $A_d$ - $A_2$ transition occurs with a jump in the layer spacing at the temperature corresponding to the dashed line. The region around thin transition point is shown on a magnified scale in the inset. The arrow mark indicates the smectic A - nematic transition point.

Xray photographs in the two phases are shown in fig. 3.5. This transition corresponds to an $A_d$-$A_2$ transition according to the nomenclature of the Bordeaux group[5] (as we have discussed in chapter 1). The characteristic feature observed at this transition is the appearance of a strong second order reflection on going over to the $A_2$ phase. It is appropriate to mention at this point that our microscopic observations on a homeotropically aligned sample taken between a slide and a coverslip showed a general shrinkage of the boundary as the sample was cooled. Presumably the number of layers between the slide and coverslip remain unaltered and as the layers expand on cooling, the boundary shrinks to conserve density. There was some enhancement in the shrinkage at the temperature corresponding to the $A_d$-$A_2$ transition. On heating the sample, the boundary again expanded.

Fig. 3.6 shows the variation of the layer spacing in the case of 12 PNCBO. The general features are similar to those of 10 PNCBO. There is a change of slope in the thermal evolution of the layer spacing at $T_{NI}-T \simeq 62^{\circ}C$, with a lowering of the rate of expansion as the sample is cooled to that temperature and a faster expansion at

(a)

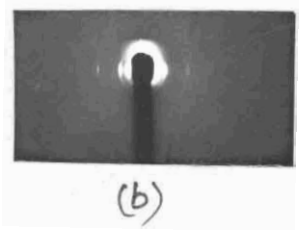

(b)

**FIGURE 3.5**

Xray photographs in (a) $A_d$ (b) $A_2$ phases of 10 PMCBB

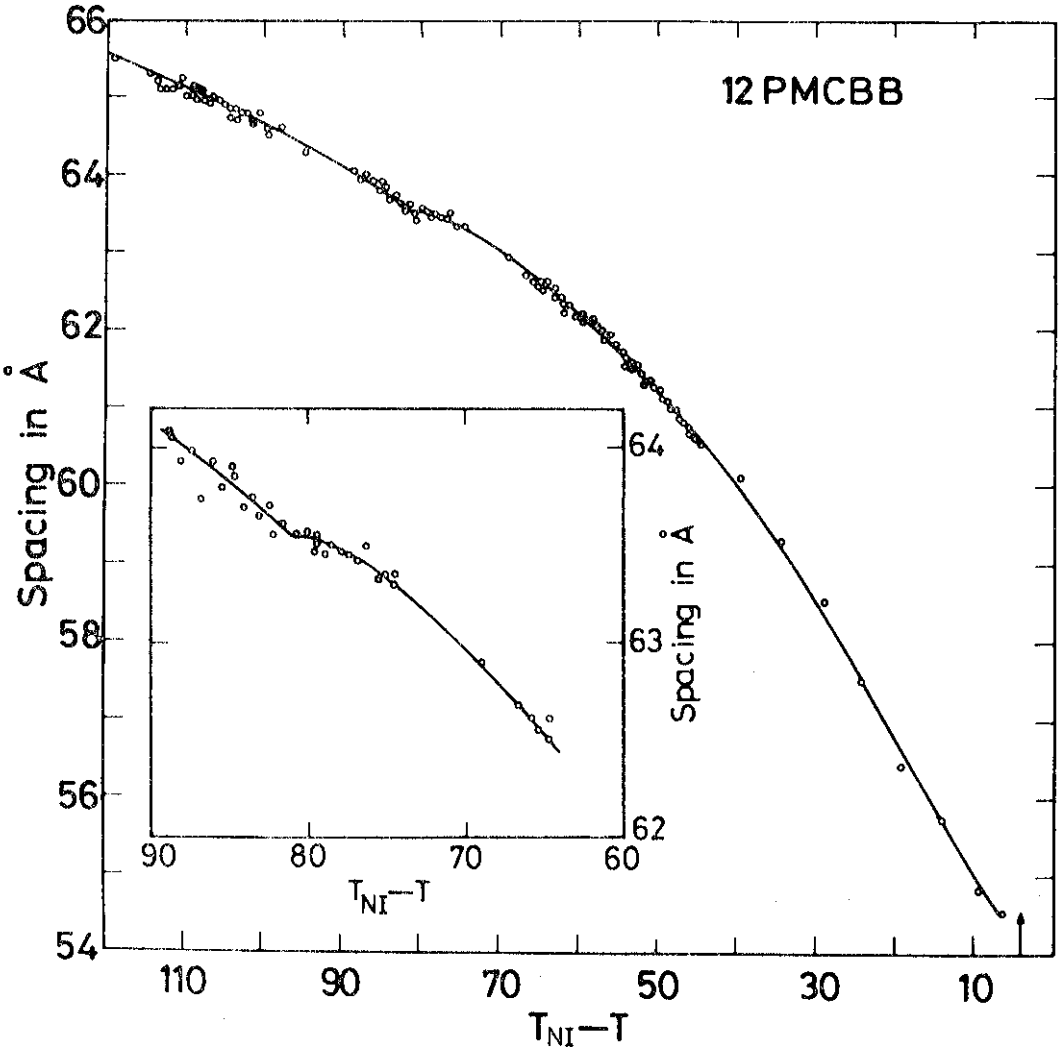


FIQ.3.6: Temperature variation of the layer spacing of 12 PMCBB. The inset shows on a magnified scale the region around the temperature at which slope change occurs. The arrow mark indicates $T_{AN}$.

lower temperatures. The second order reflection is strong at lower temperatures. This trend is reminiscent of that shown by 10 PNCBB, but without any jump in the layer spacing. It most probably represents a second order $A_d$-$A_2$ transition. However, we could not locate this transition on the DSC curves.

The temperature variations of the layer spacings in 9 PNNBB, 10 PNNBB and 12 PNNBB are shown in figs.3.7-3.9. In 9 PNNBB (fig. 3.7), the curvature appears to change sign at $T_{A/I}$, the rate of expansion becoming larger at lower temperatures in the A phase. The latter trend is particularly obvious in 10 PNNBB (fig.3.8). Indeed from a comparison with the data on 10 PNCBB (fig. 3.4) some striking differences are seen when the cyano end group is replaced by the nitro end group: (a) the curvature of the thermal dependence of the layer spacing changes sign; and (b) $A_d$-$A_2$ transition is absent in the nitro compound. Since the molecular lengths in the two cases are practically the same, it is also clear that the bilayer spacing in the nitro compound is somewhat lower than in the cyano compound. In the case of 12 PNNBB (fig.3.9) the curvature changes sign in the A phase, the rate of expansion becoming lower at the

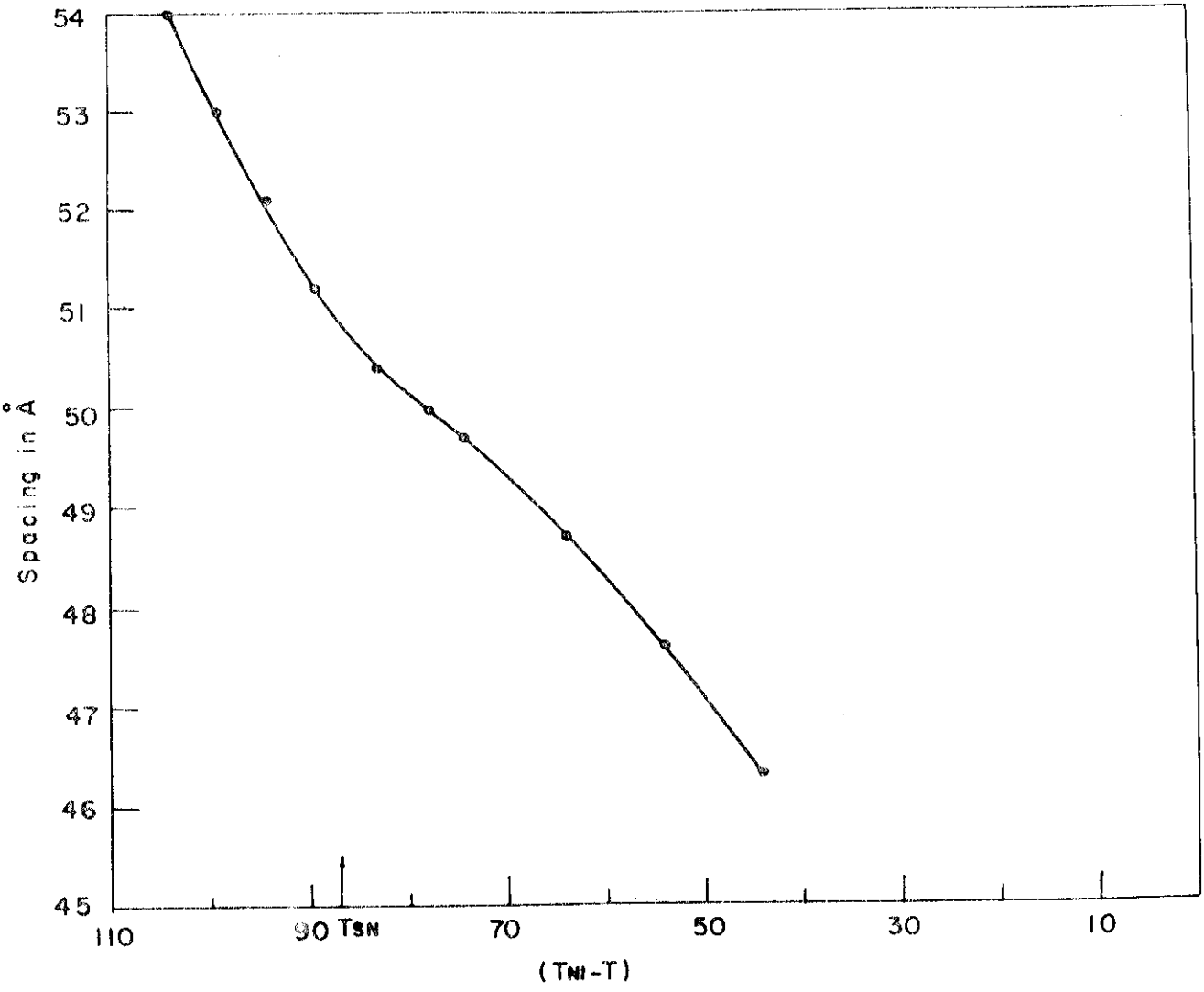


**FIG.3.7: Temperature variation of the layer spacing of 9PMNBB.**

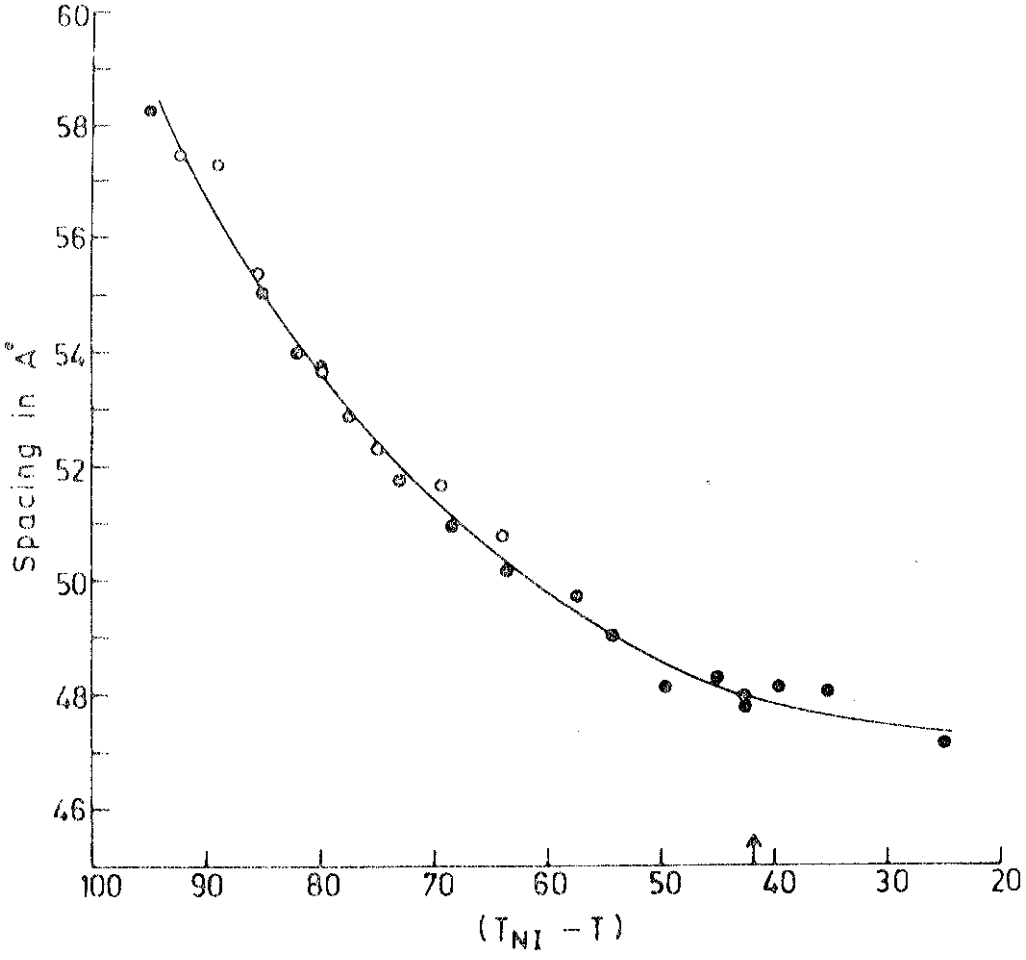


**FIG.3.8:** **Temperature variation of the layer spacing of 10 PMNBB. The arrow mark indicates $T_{AN}$.**

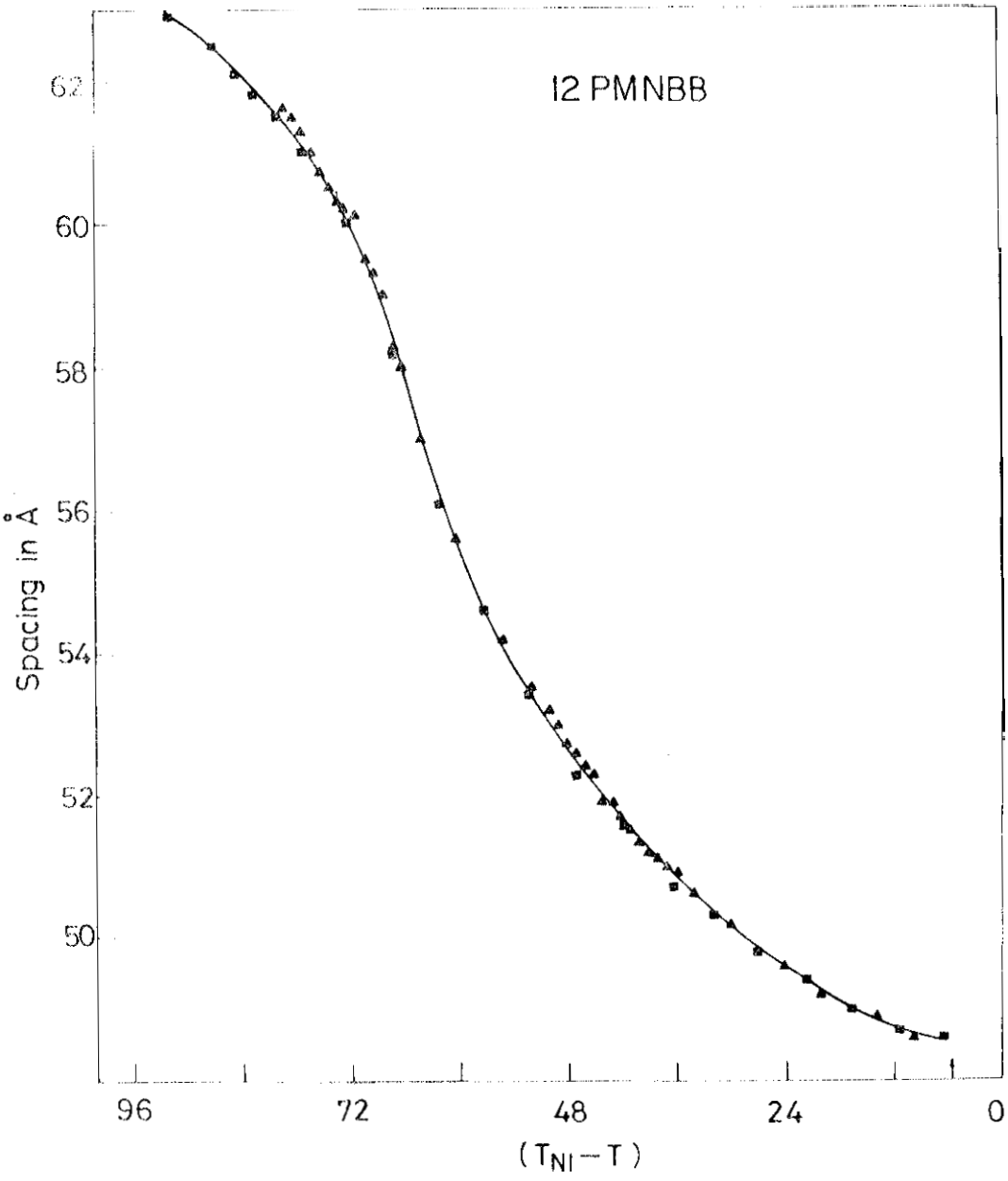


**FIGURE 3.9**

**Temperature variation of the layer spacing of 12 PMNBB. The arrow mark indicates $T_{AN}$.**

lowest temperatures for which measurements could be taken. In all these cases, the second order reflection is seen only at very low temperatures: the intensity of second order reflection gradually increasing with decrease of temperature In all the nitro compounds, the layer spacing evolves continuously with temperature, without any jump or change of slope.

Figs. 3.10-3.12 show the results on 10 PMeOCBB, 11 PMeOCBB and 12 PMeOCBB respectively. Again there is a fairly large and continuous expansion in the layer spacing as the temperature is lowered, without any indication of jump or change of slope. The second order reflection was very difficult to get even at the lowest temperatures.

The results on 11 CPMeOBB and 12 CPMeOBB, which are obtained by interchanging the end groups of 11 PMeOCBB and 12 PMeOCBB respectively, are depicted in figs. 3.13 and 3.14 respectively. In both the cases, the layer contracts by 1-2 Å as the temperature is raised by $\sim 70^{\circ}$, the rate of contraction becoming negligible close to $T_{AN}$. The molecular lengths of the two homologues measured using the Dreiding models are $\sim 33.6$ Å and $\sim 35$ Å respectively. The measured layer spacings indicate

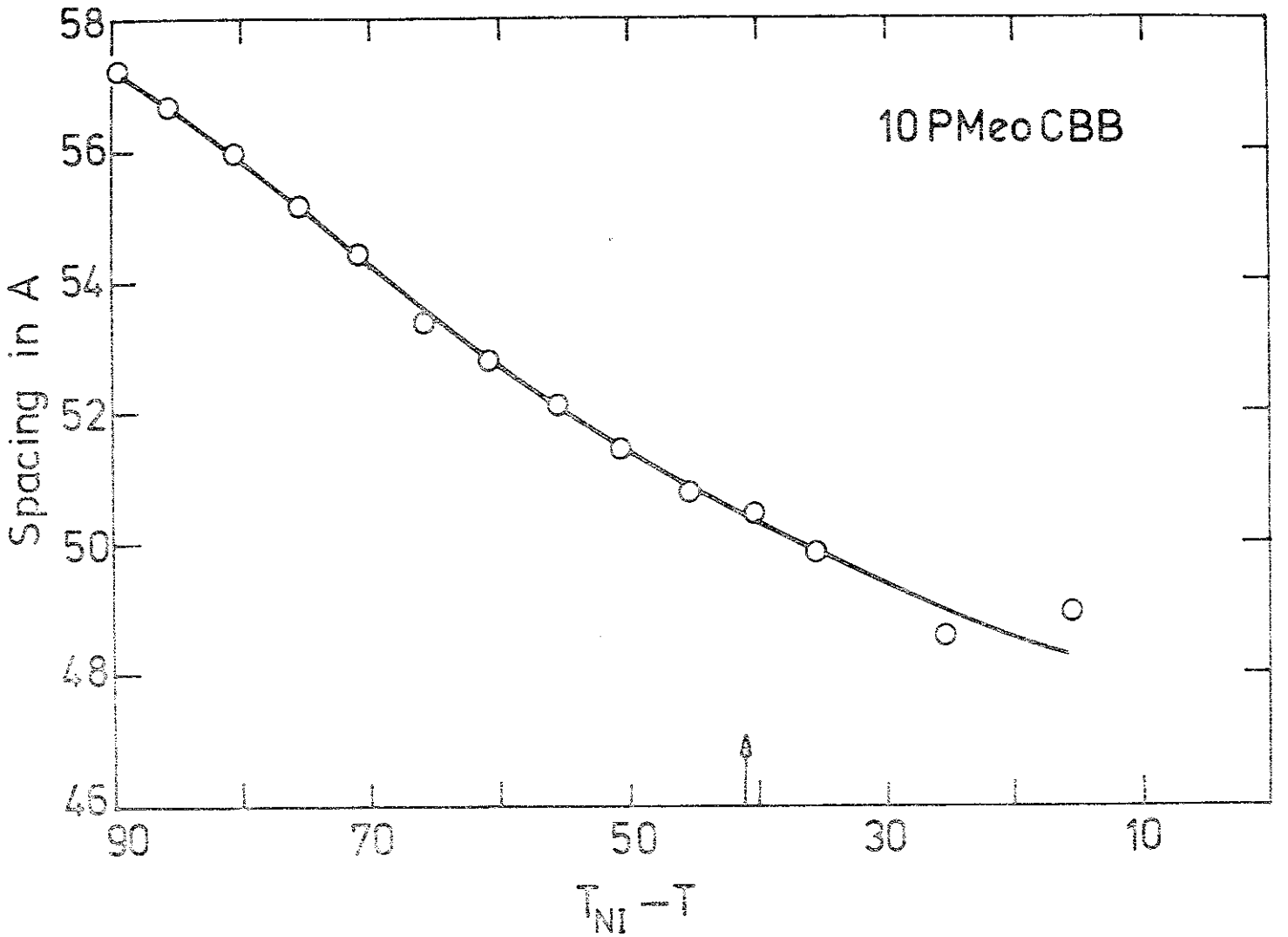


FIG.3.10: Temperature variation of the layer spacing of 10 PMeOCBB. The arrow mark indicates $T_{AN}$.

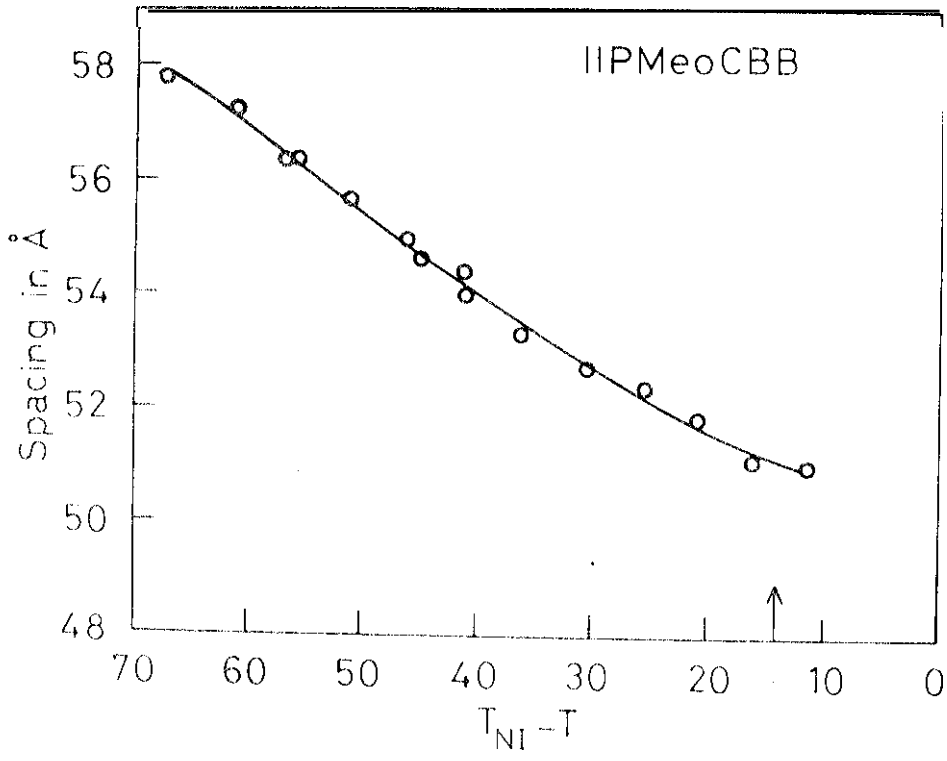


**I .1 Temperature variation of the layer spacing of 11 PMeOCBB. The arrow mark indicates $T_{AN}$ .**

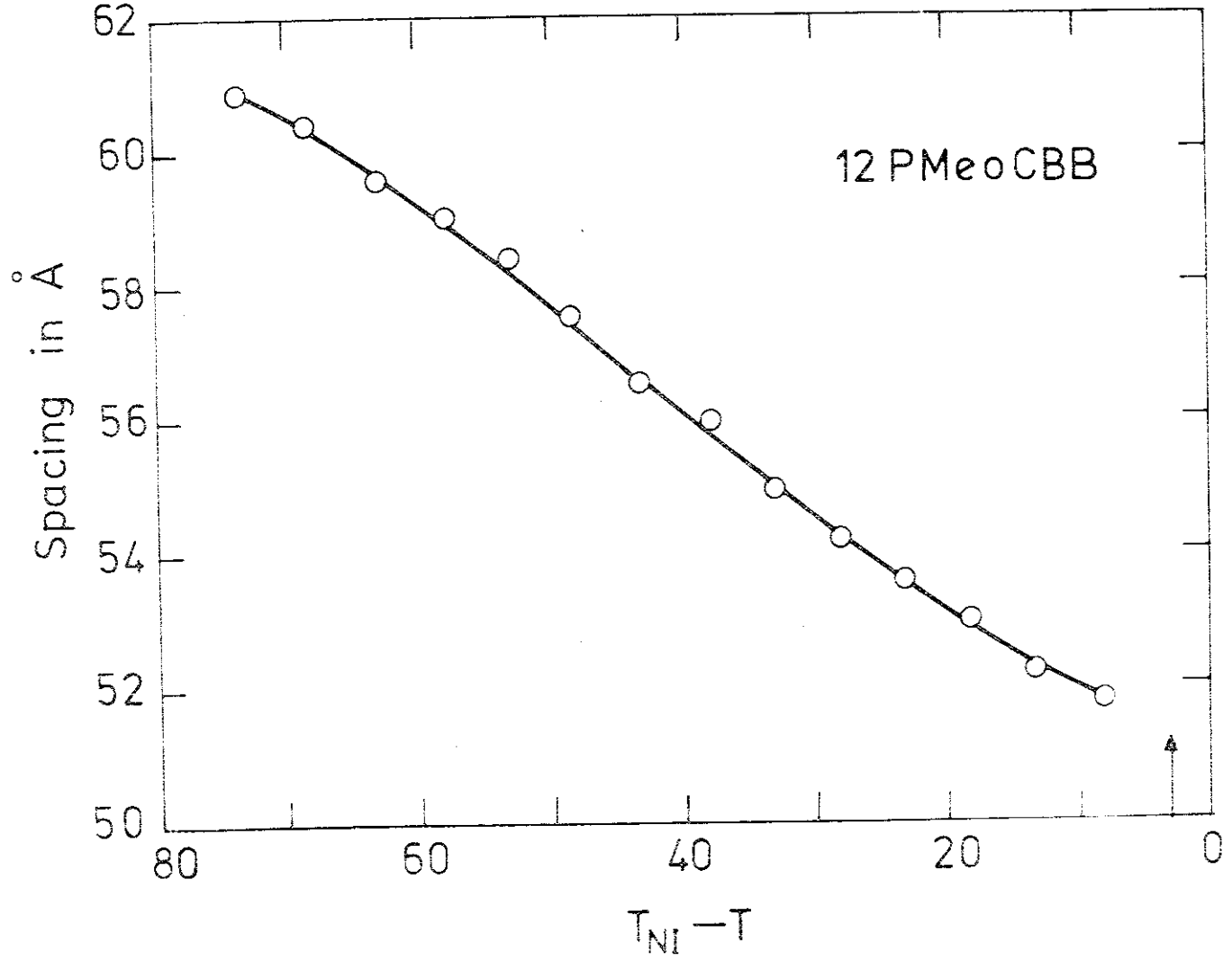


FIG.3.12: Temperature variation of the layer spacing of 12 PMeOCBB. The arrow indicates $T_{AN}$.

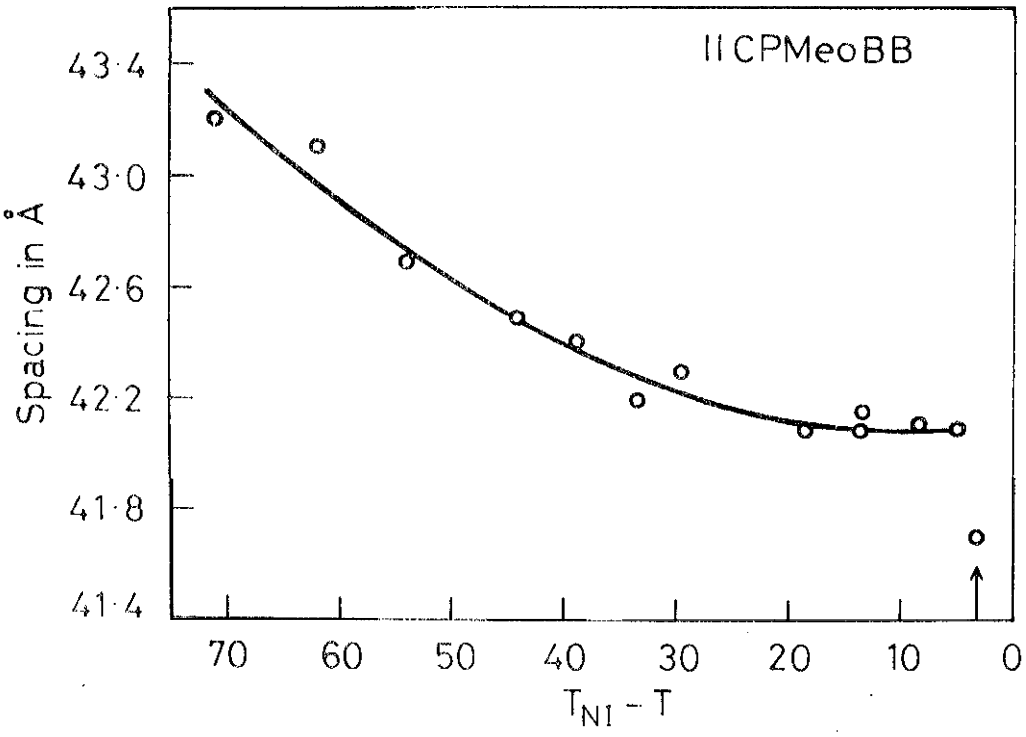


**FIQ.3.13:** Temperature variation of the layer spacing of 11 CPMeOBB. The arrow mark indicates $T_{AN}$.

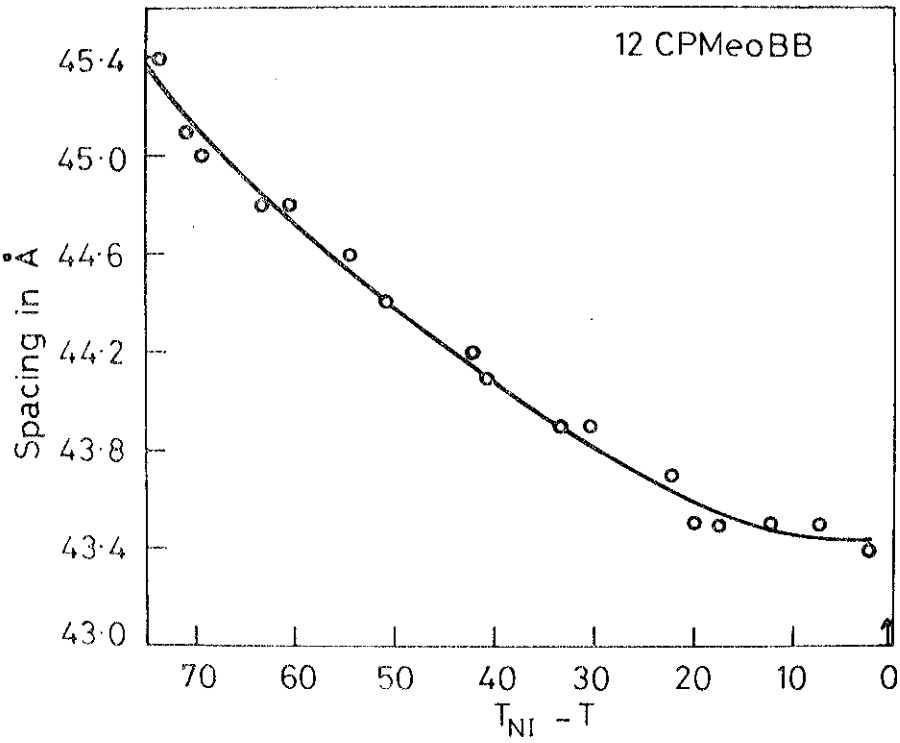


FIGURE 3.14

Temperature variation of the layer spacing of 12 CPMeOBB The arrow mark indiastos $T_{AN}$ .

interdigitated partial bilayers with $\underline{d} \simeq 1.3\underline{l}$ at the lowest temperature of measurement in the two cases. The bilayer spacings are thus much smaller than the corresponding nFMeOCB compounds which have $\underline{d}$ values $\simeq 1.7\underline{l}$ at low temperatures.

Though the temperature variation of $\underline{d}$ is by no means linear in most cases studied, it is interesting to compare the average values of $(\Delta\underline{d}/\Delta T)$ over the entire range of measurement in all the cases. The results are shown in table 3.2. The values increase *fur* the higher homologues. This trend is similar to that found earlier by Cladis et al.[17] in the case of 4-n-alkoxyphenyl-4'-cyanobenzoates which have one ester linkage group whose longitudinal component of the dipole moment opposes that of the cyano end group. When the compound has two ester linkage groups (as in the compounds that we have studied), but without any lateral substituent, one finds A-A transition in many homologues of both the cyano and nitro compounds,[5] and further the layer spacing does not appear to be strongly temperature dependent. However, when one of these cyano compounds (DB7) is mixed with octyloxycyanobiphenyl the $A_d$-$A_2$ transition becomes weaker as the 8 OCB concentration is increased, and the layer spacing also becomes strongly temperature dependent.[18]

## Table 3.2

Average rate of thermal expansion of the layers

| | $\Delta d/\Delta T$ in Å/°C | | | |
|---|---|---|---|---|
| | n = 9 | n = 10 | n = 11 | n = 12 |
| nPMCBB | -0.05 | -0.07 | - | -0.1 |
| nPMNBB | -0.13 | -0.16 | - | -0.17 |
| nPMeOCBB | - | -0.12 | -0.13 | -0.14 |
| nCPMeOBB | - | - | -0.019 | -0.027 |
| nPMeOBrBB | - | - | + 0.06 | +0.05 |

An examination of our results clearly indicates that when the dipole moments of the ester linkages oppose that of the terminal polar group (as in nPMCBB, nPMNBB, nPMeOCBB), the compounds show (i) relatively large bilayer spacing $d \gtrsim 1.6$ and (ii) a fairly large expansion of the spacing as the temperature is lowered in the A phase. If the dipole moments of the ester linkages are aligned parallel to that of the end polar group (as in nCPMBB and nCPMeOBB), the bilayer spacing is considerably smaller ($\simeq 1.3\lambda$) and the thermal dependence of the spacing is also weaker.[19]

One possible interpretation of the strong thermal dependence of $d$ in all the cases is that the interdigitation in the bilayer varies continuously with temperature (fig. 3.15). A more plausible interpretation can, however, be obtained by considering the mutual interactions between a pair of molecules, as we have discussed in a paper presented at the Ninth International Liquid Crystal Conference, Bangalore.[20] For the sake of comparison, we shall first consider a pair of nCPMBB molecules (Fig. 3.16a). Since the longitudinal components of both the ester groups are aligned parallel to the dipole moment of the cyano group, the interaction energy can be minimized by a complete overlap of the aromatic cores as shown in fig.3.16a. On the other hand, in nPMCBB compounds a similar overlap of the aromatic cores (fig.3.16b)

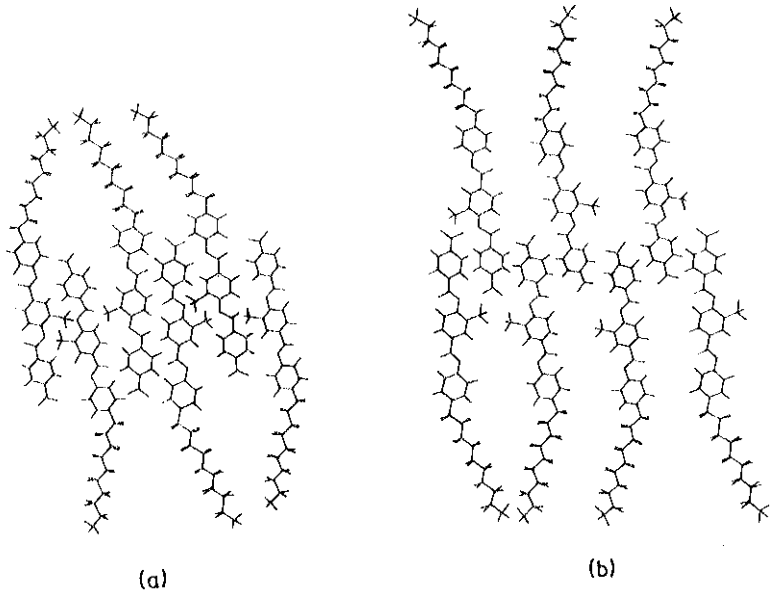


FIGURE 3.15

Schematic drawings of a possible structure of the bilayer in (a) higher temperature range, and (b) lower temperature range of the A phase. Actually, the three phenyl rings are not likely to be coplanar.

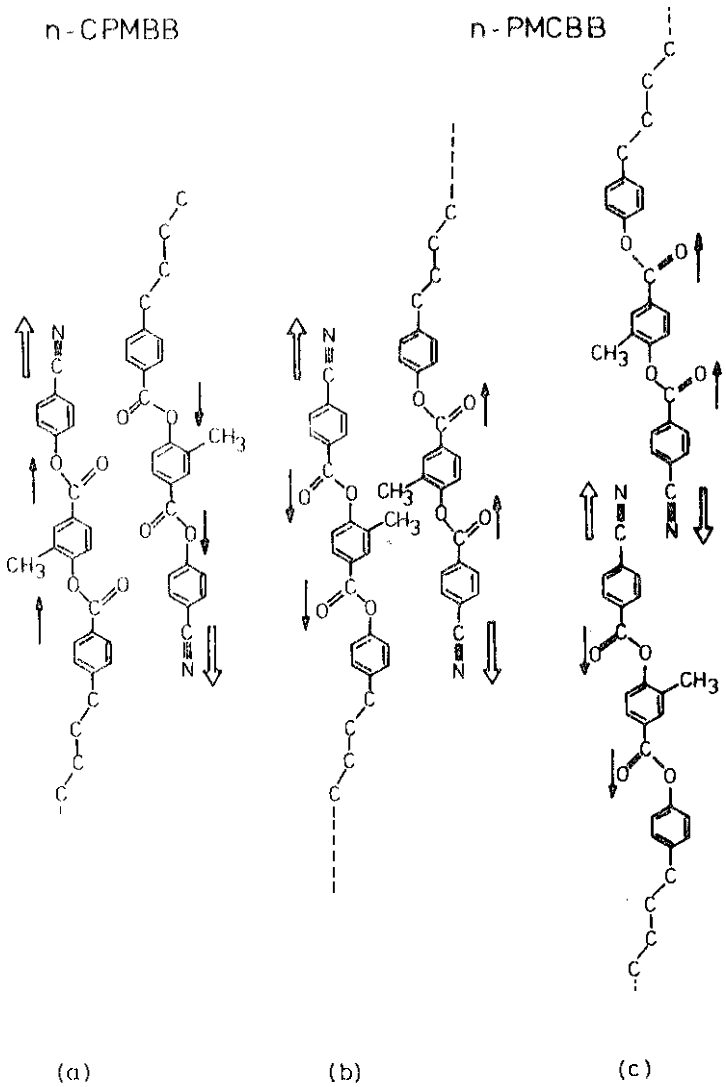


**FIff.3.16:** Schematic diagrams showing the disposition of various dipolar groups of a pair of (a) n--CPMBB, (b) n-PMCBB molecules with an overlap of the aromatic cores, and (c) a pair of n-PMCBB molecules with an overlap of the polar end groups.

would result in strong repulsive interactions b%* — *&%@ dipole ==—% of the cyano @— of one molecule and that of one of the ester groups of the neighbouring molecule. The dipolar contribution to the interaction energy would be minimized by an overlap of the two molecules only near the cyano end groups as shown in fig.3.16c. Since the dipole moment of the cyano end group is $\simeq$ 4D, the dipolar interaction energy ($\sim \mu^2/r^3$) is a few times the thermal energy $k_B T$. Further, since this interaction Is confined to one end of the molecule, it is clear that the structure as shown in fig.3.16c should be rather fragile. As the temperature is raised, the structure can easily break up. This physical model can easily explain the rapid decrease in the layer spacing as the temperature Is raised. As the molecules become heavier with longer chains, the structure shown Pa fig.3.16c can be expected to become more fragile accounting for the larger coefficients of thermal contraction of the layer spacing (table 3.2). The lateral substituent also makes the molecules bulkier adding to the fragility of the structure Further, the intermolecular repulsions of the single molecules (as in fig. 3.16b) which break away from the structure shown in fig. 3.16c would be smaller than in compounds without the lateral substituent. This may

account for the relatively stronger thermal contraction observed in compounds with the lateral substituents than in the compounds without lateral substituents. Further, this interpretation accounts for the somewhat larger thermal contraction of nPMeOCBB compounds compared to those of nPNCBB compounds as the methoxy group is bulkier than the methyl group. nPNBB compounds have the largest thermal contraction of the layer spacings, even though the longitudinal dipole moment of the $NO_2$ group is almost the same as that of the cyano group. Obviously the interactions between the lateral components of the dipole momentsof the NO bonds would be repulsive on the average and would contribute to a reduction in the attractive interactions between the end groups.

For the sake of comparison we have also studied the temperature variations of layer spacings of 11 PMeOBrBB and 12 MeOBrBB in which the cyano end group of nPMeOCBB is replaced by a bromine atom leading to a large decrease in the polarity of the terminal group. As shown in figs. 3.17 and 3.18, the layer spacing now corresponds to one molecular length, i.e., the bromine compounds form a monolayer smectic A phase. Further, the layer spacing expands by $\sim$ 1-2 Å as the temperature is raised by $\sim$ 30-40°C, and the layer expansion coefficient increases as $T_{AN}$ is

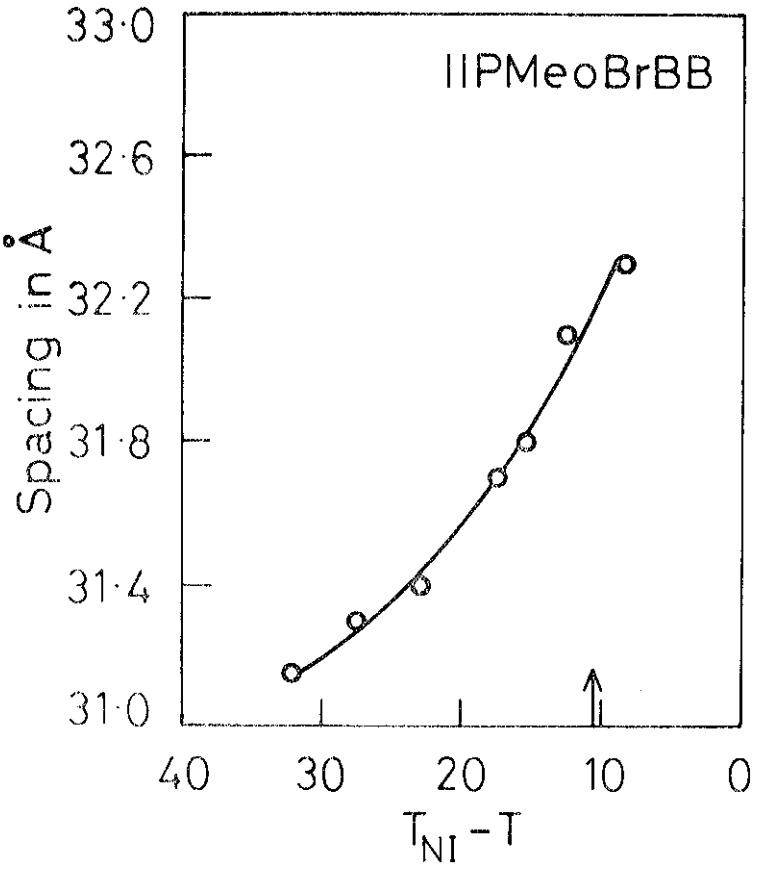


**FIGURE 3.17**

Temperature variation of the layer spacing of **11** PMeOBrBB. The arrow mark indicates $T_{AN}$ .

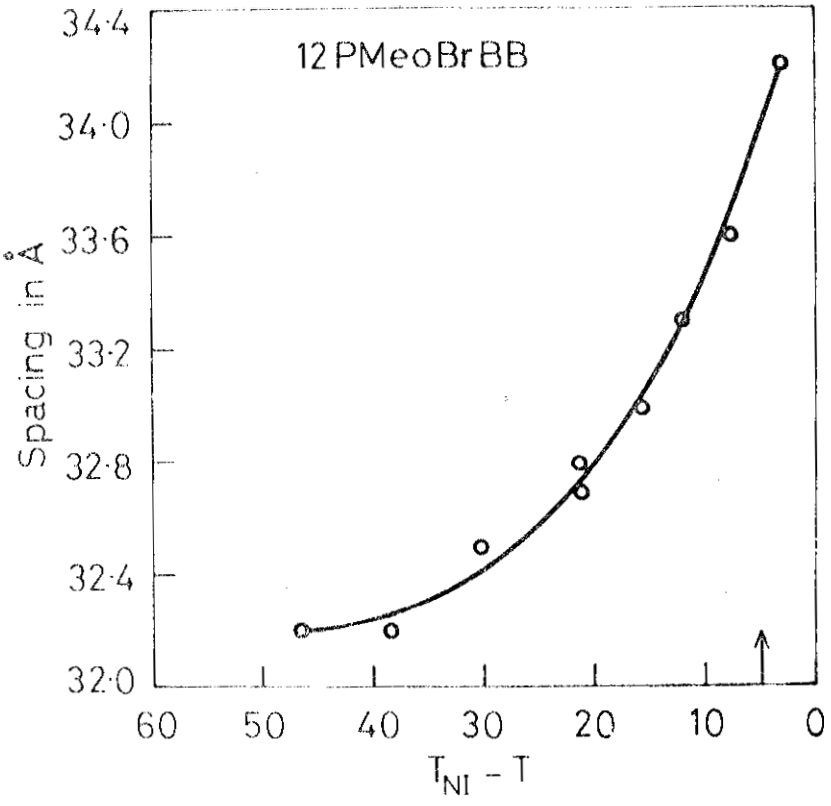


**FIGURE 3.18**

**Temperature variation of the layer spacing of 12 PMeOBrBB. The arrow mark indicates $T_{AN}$.**

approached. This expansion appears to be much larger than that observ in earlier studies on monolayer smectics[21,22] which were made on compounds without any lateral substituent. Our own measurements on the monolayer compound B011 (table 3.1, fig.3.1) which does not have any lateral substituent is shown in fig.3.19 and this compound also exhibits only a very weak layer expansion with mperature. The layer expansion coefficient $(\frac{1}{d}\frac{\Delta d}{\Delta T}) \simeq 20 \times 10^{-4}$ in nPMeOBrBB near $T_{AN}$ while it is about 10 times smaller in B011. We believe that this difference is due to the presence of a bulky methoxy substituent in the former compounds, leading to a weaker attractive interaction between the aromatic moeities. Thus the layer expansion coefficient is of the order of volume expansion coefficient observed near A-N transition point of several compounds.[23] On the other hand, the attractive forces between the aromatic parts of molecules like B011 are much stronger and the layer expansion coefficient is weak and in such cases, the volume expansion should therefore be accounted for by the creation of voids in the plane of the layers. As de Vries[22] has noted, the average lateral spacing in such a system increases with temperature more rapidly in the A phase compared to that in the isotropic phase.

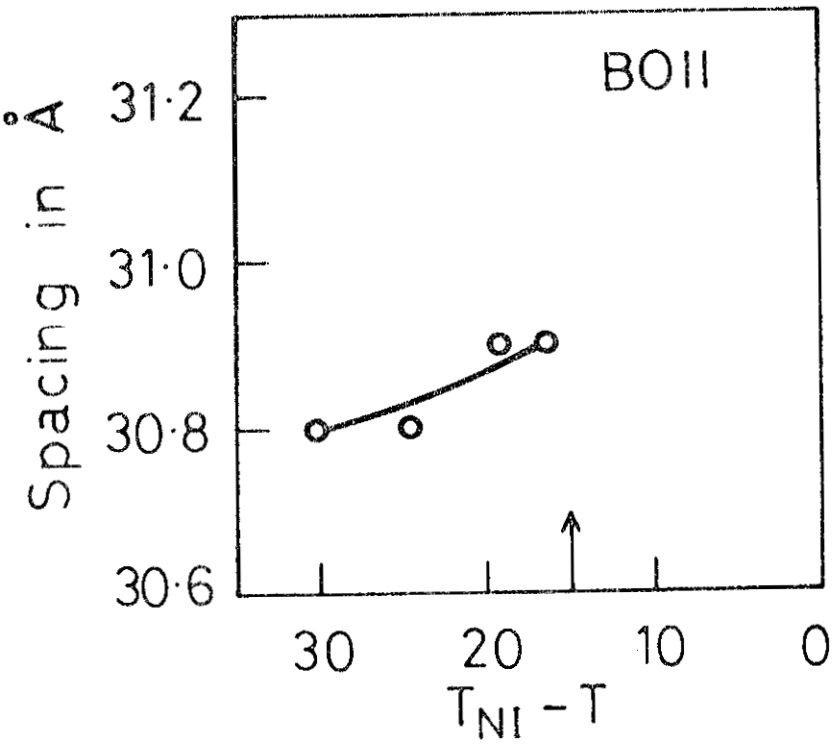


FIGURE 3.19

**Temperature variation of the layer spacing of BOll. The arrow mark indicates $T_{AN}$.**

The thermal contraction of bilayer in the A phase of nClMeOBB means that the molecular pairs with interdigitation of the aromatic parts are also not strongly bound in these compounds. As we discussed earlier the case of nFMeOBrBB) the mutual interactions are not very strong due to the presence of the lateral methoxy group. As the temperature is raised, in nClMeOBB compounds the pairs can break up, giving rise to the layer contraction. However, there should also be an opposing trend, since, as in the case of nFMeOBrBB, the volume expansion should lead to a layer expansion. At lower temperatures, the latter effect is much smaller than the contraction effect due to the breaking up of pairs. As the temperature approaches $T_{AN}$, the two effects appear La balance each other leading to a levelling off in the layer spacing (figs. 3.13 and 3.14). On the other hand, in the case of nFMeOClBB, the breaking up effect on the large bilayer spacing is so strong that the volume expansion hardly affects the trend in the thermal evolution the layer spacing (figs. 3.10-3.12).

It is interesting at this point to refer to an earlier study[19] on some nClMeBB compounds (table 3.1) which exhibit the reentrant nematic phase. These have a lateral methyl group which is smaller than the methoxy

group of nCPMeOHB compounds. Temperature variations of layer spacings in the A phase of eleventh and twelfth homologues of the former series are reproduced from ref.19 in figs.3.20 and 3.21 respectively. They exhibit layer contraction as the temperature is raised from $T_{AN_R}$, and with further increase of temperature exhibit a broad minimum, and then an expansion of the bilayer spacing. Probably the breaking up of pairs is responsible for the low temperature behaviour and the large volume expansion as T approaches $T_{AN}$ leads to the high temperature behaviour.

Coming back to the large layer spacing contraction exhibited by the nTMCHB and nTMOHB compounds, Guillon et al.[24] have analysed our data on the 10th members of both the series to calculate the mean areas occupied by the paraffin chains. It is easy to see that this area S is given by

$$S = \frac{2V}{dN}$$

where V is the molar volume, d the layer spacing and N the Avagadro number. Since the densities of these compounds have not been measured, they use variations which are 'typical' of liquid crystals: V = 500 + 0.4t (°C) and calculate S (fig. 3.22).

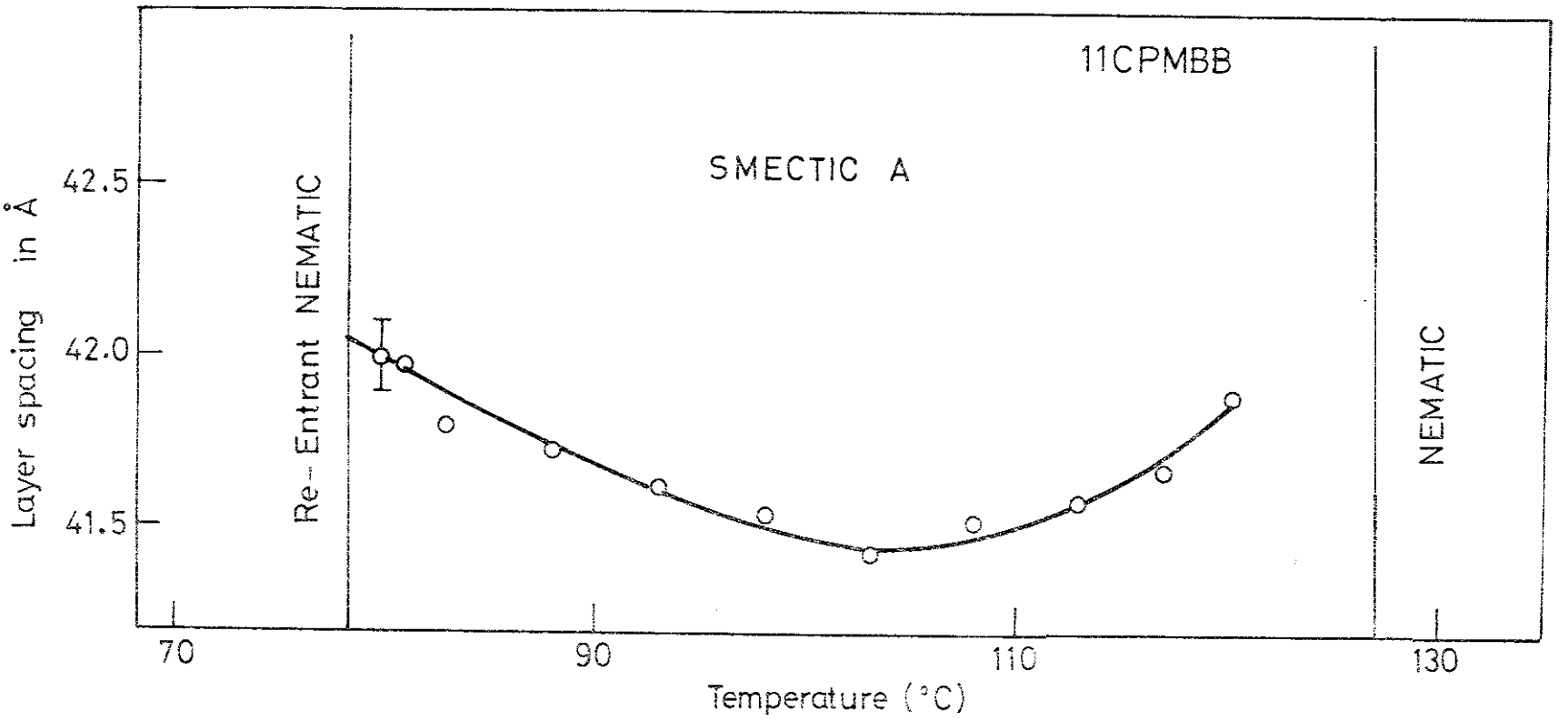


**FIG.3.20: Temperature variation of the layer spacing of 11 CPMBB. (Reproduced from ref. 19)**

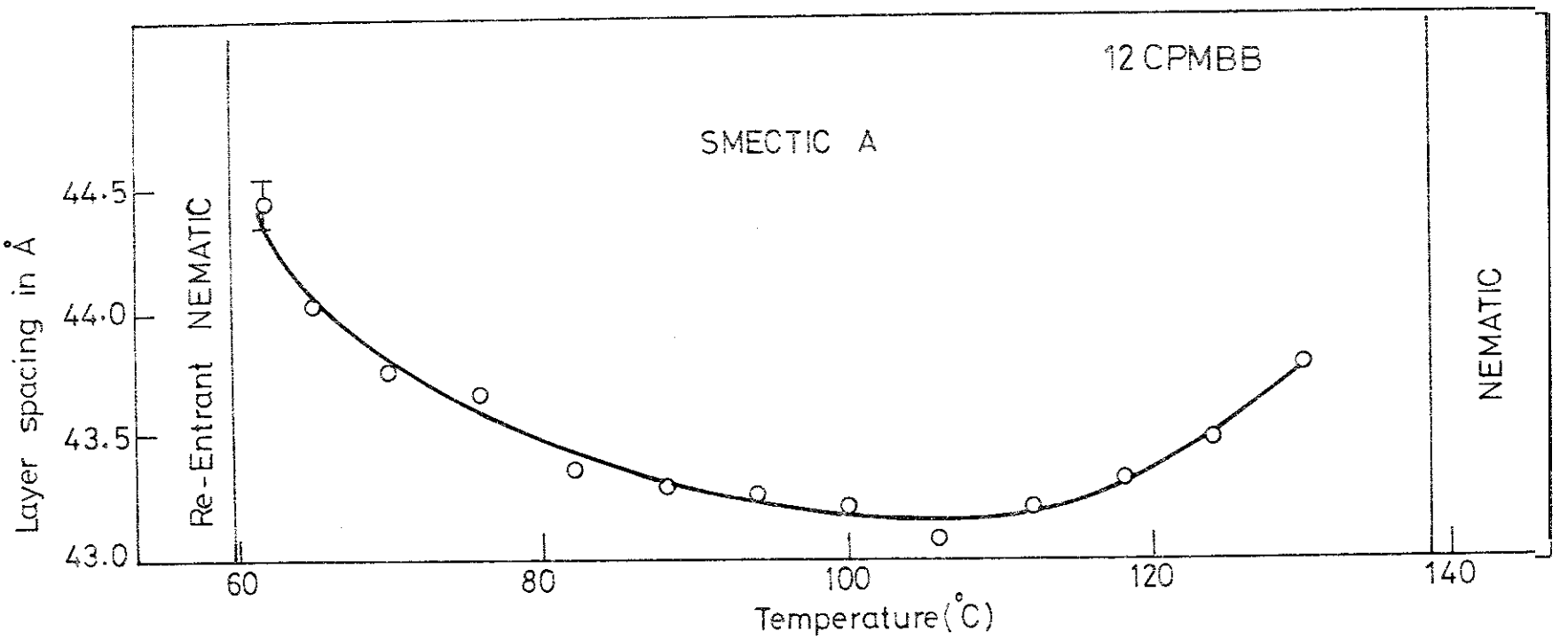


**FIGURE 3.21**

**Temperature variation of the layer spacing of 12 CPMBB.(Reproduced rom ref.19)**

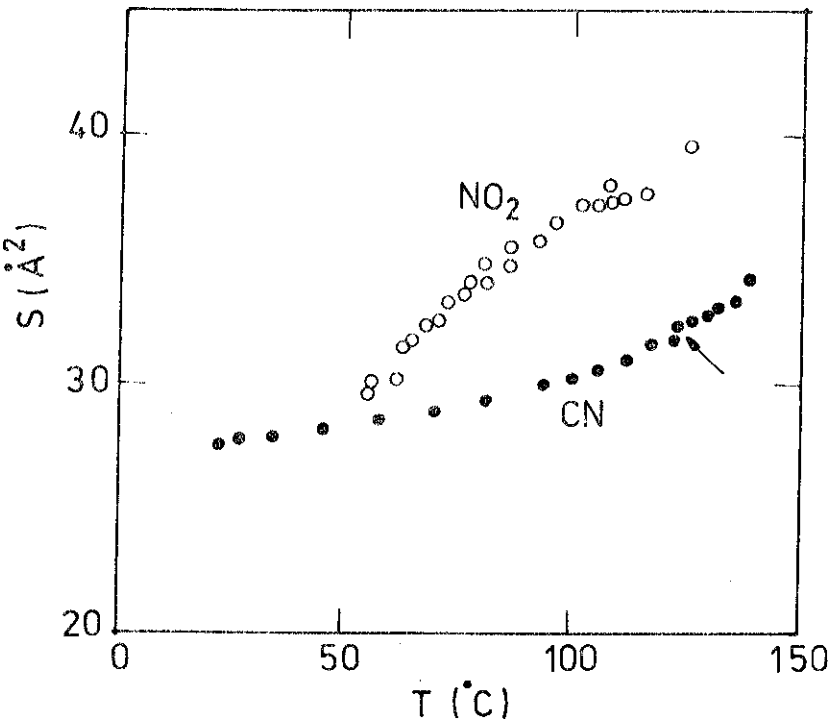


FIGURE 3.22

Molecular area of paraffin chains as a function of temperature. (Reproduced from ref. 24).

Guillon and Skoulios[25] have also made a simple calculation using the same physical idea that we discussed earlier. Assuming that the interaction energy of a pair associated as shown in fig. 3.16b as $E_s$ and that corresponding to fig. 3.16c as $E_h$, the Boltzmann probabilities of finding the molecular pairs in the two configurations are: $P_s = 1 - P_h = \exp(-E_s/k_BT)$, $P_h = \exp(-E_h/k_BT)$. If $\tau$ is the degree of head to head association (as in fig. 3.16c), $(P_h/P_s) = (\tau/1-\tau) = \exp(-\delta E/k_BT)$ where $\delta E = E_h - E_s$ and let $e = \delta E/k_BT$.

Further, assuming that the head to head pairs have a length = $2l$, where $l$ is the length of a single molecule and that their molecular area is very close, if not identical, to that of the single molecules, they have calculated the bilayer spacing $\underline{d}$: $(\underline{d}/l) = 2/(2-\tau)$. The results are shown in fig. 3.23. It is seen that the trend for $e = -0.5$ is similar to that for the nFMeBB compounds, while the nFMeCBB compounds have trends for $e = -2$ or more, with the nFMeOCBB compounds have trends for $e$ values somewhere in between. We have already discussed the origin of the differences in the interaction energies for these three series.

The $A_d - A_2$ transition seen in 10 FMeCBB is similar to the one discussed by Frost and Barion[26] in terms of a

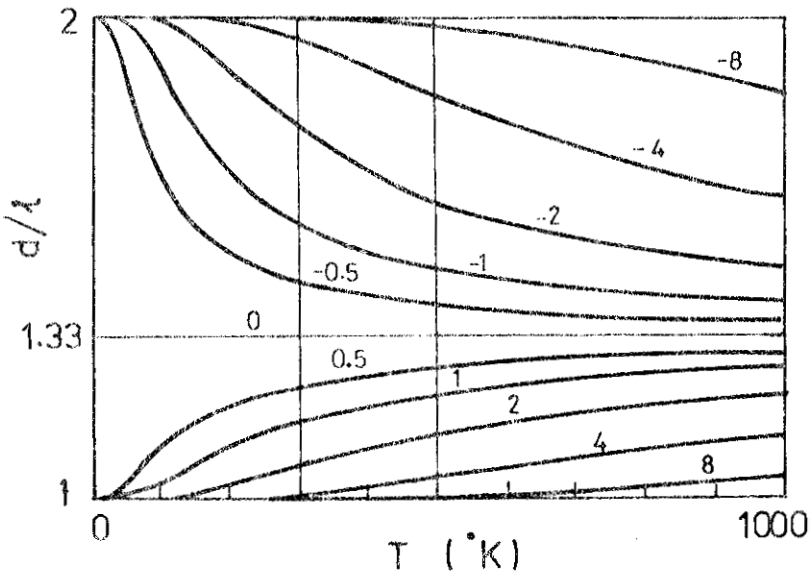


FIGURE 3.23

**Temperature dependence of the ratio of the layer thickness (d) to the molecular length (λ) us a function *of* $\epsilon = \delta E/k_B T$. (Reproduced from ref. 25).**

general model that they have developed for the 'frustrated' smectics exhibited by compounds with strongly polar end groups. It is a phenomenological Landau type theory with <u>two</u> order parameters; corresponding to (i) the mass density wave and (ii) the dipolar potential $\phi$ (which is defined by $P(r) = \frac{1}{4\pi}\nabla\phi$, where $P(r)$ is the dipole density). The mass density wave is supposed to have an optimum wavelength $\simeq l$, the molecular length while the electric potential has an optimum wavelength $\simeq l'$, the thickness of a molecular pair. The form of the effective free energy depends on the ratio $l'/l$. Using the model, they are able to give a description of the many smectic phases like, $A_d$, $A_2$, $A_1$ and $\tilde{A}$ exhibited by compounds with highly polar end groups. In particular, they have also given a phenomenological description of the $A_d$ - $A_2$ transition of the type observed in 10 PNCBB.

In conclusion, the mutual disposition of permanent dipolar groups, in the molecules of mesomorphic compounds which have strongly polar end groups, has a profound influence on the bilayer structures and the nature of phases exhibited by them. If the cyano or nitro dipole moment is parallel to the ester dipole moments, the compounds have a partial bilayer spacing $\simeq 1.4\,l$ and may

show reentrant phases. If the ester dipole moments oppose that of the terminal polar group, the compounds have large bilayer spacings. If the polar group is replaced by the relatively weakly polar bromine atom, we obtain monolayer smectics. The bulky lateral methyl group decreases the intermolecular interactions, thus leading to a large thermal influence on the layer spacings. Thus the nPMCBB compounds exhibit a large contraction of the spacing with temperature, the $10^{th}$ and $12^{th}$ members having an $A_d - A_2$ transition as well. The bulkier methoxy lateral group of nPMeOCBB leads to larger contractions. The weaker interactions between the nitro groups result in a rather easy breaking up of the bilayer structure of nPMNBB compounds. The nCPMBB and nCPMeOBB compounds also exhibit thermal variations of the layer spacings dominated by the breaking up of a partial bilayer structure at low temperatures and the effect of volume expansion of the medium at higher temperatures (close to the AN transition point). The monolayer bromo compounds also exhibit an expansion of the layer spacings, which is much stronger than in the case of monolayer compounds like 8O11 which do not have a lateral substituent.

In the next chapter, we will study the strong thermal influence on the dielectric properties of these compounds.

REFERENCES


1 A.J.Leadbetter, R.M.Richardson and C.N.Colling, J. de Phys. 36, C1-37 (1975).

2 N.V.Madhusudana and S.Chandrasekhar, Proc.Int.Liq. Cryst.Conf., Bangalore, 1973, Pramana Suppl. 1, p.57.

3 W.L.McMillan, Phys. Rev. A4, 1238 (1971).

4 W.Maier and A.Saupe, Z.Naturforsch. 13a, 564 (1958); ibid., 14a, 882 (1959); ibid., 15a, 287 (1960).

5 F.Hardouin, A.M.Levelut, G.Sigaud, Nguyen Huu Tinh and M.F.Achard (invited talk) presented at the Ninth Int.Liq.Cryst.Conf., Bangalore (1982).

6 A.J.Leadbetter, J.C.Frost, J.P.Gaughan, G.W.Gray and A. Mosley, J.de Phys. 40, 375 (1979).

7 J.E.Lydon and C.J.Coakley, J.de Phys. 36, C1-45 (1975).

8 P.E.Cladis, Phys.Rev.Lett. 35, 48 (1975).

9 N.V.Madhusudana, B.K.Sadashiva and K.P.L.Moodithaya, Curr. Sci. 48, 613 (1979).

10 F.Hardouin, G.Sigaud, M.F.Achard and H.Gasparoux, Solid State Commun. 30, 269 (1979).

11 F.Hardouin, A.M.Levelut, J.J.Benattar and G.Sigaud., Solid State Commun. 33, 337 (1980).

12 A.M.Levelut, R.J.Tarento, F.Hardouin, M.F.Achard, and G.Sigaud, Phys.Rev. A24, 2180 (1981).

13 M.Subramanya Raj Urs (to be published).

14 M.Subramanya Raj Urs and V.Surendranath, Mol.Cryst.Liq. Cryst. 99, 279 (1983).

15 P.E.Cladis (private communication)

16 F.Hardouin, A.M.Levelut and G.Sigaud, J.de Phys. 42, 71 (1981).

17 P.E.Cladis, P.L.Finn and J.W.Goodby, Presented at the American Chem.Soc.Meeting, Las Vegas, 1982.

18 A.M.Levelut, B.Zaghloul and F.Hardouin, J.de Phys.Lett. 43, L-83 (1982).

19 S.Chandrasekhar, K.A.Suresh and K.V.Rao, Proc.Int. Liq.Cryst.Conf., Bangalore, 1979. Liquid Crystals, Ed. S.Chandrasekhar, Heyden,London (1980) p.131.

20 N.V.Madhusudana, B.S.Srikanta and M.Subramanya Raj Urs, Presented at the Ninth Int.Liq.Cryst.Conf., Bangalore, 1982, Mol.Cryst.Liq.Cryst. 97, 49 (1983).

21 S.Diele, P.Brand and H.Sackmann, Mol.Cryst.Liq.Cryst. 16, 105 (1972).

22 A. de Vries, Mol. Cryst. Liq. Cryst. 20, 119 (1973).

23 D.Demus and R.Rurainski, Z.Phys.Chimie (Leipzig), 253, 53 (1973).

24 D.Guillon, G.Poeti and A.Skoulios, Mol.Cryst. Liq. Cryst.Lett. 92, 35 (1983).

25 D.Guillon and A.Skoulios, Mol.Cryst.Liq.Cryst.Lett., 92, 1 (1983).

26 J.Prost, and P.Barois, J.Chemie Physique, 80, 65 (1983).

27 B.K.Sadashiva, Mol. Cryst. Liq. Cryst. 55, 135 (1979).